Characteristics of Internal Transport Barrier under Reactor Relevant Condition in JT-60U Weak Shear Plasmas

H. Takenaga[1], N. Oyama[1], H. Urano[1], Y. Sakamoto[1], K. Kamiya[1], Y. Miyo[1], T. Nishiyama[1], T. Sasajima[1], K. Masaki[1], A. Kaminaga[1], H. Ichige[1], J. Bucalossi[2], V. Marty[2], S. Ide[1], Y. Koide[1], Y. Kamada[1] and the JT-60 Team

[1] Japan Atomic Energy Agency, Naka, Ibaraki-ken 311-0193, Japan
[2] Association Euratom-CEA, CEA Cadarache, CEA-DSM-DRFC, F-13108 St Paul lez Durance, France

e-mail contact of main author: takenaga.hidenobu@jaea.go.jp

Abstract. Characteristics of internal transport barrier (ITB) have been investigated under reactor relevant condition with edge fuelling and electron heating in JT-60U weak shear plasmas. High confinement was sustained at high density with edge fuelling by shallow pellet injection or supersonic molecular beam injection (SMBI). The ion temperature (T_i) in the central region decreased even with edge fuelling. The T_i decrease with edge fuelling was larger inside the ITB than that outside the ITB, which can be described by cold pulse propagation using the ion thermal diffusivity (χ_i) estimated from power balance analysis in the SMBI case. By optimizing the injection frequency and the penetration depth, the decreased T_i was recovered and good ITB was sustained with enhanced pedestal pressure. The T_i-ITB also degraded significantly when stiffness feature was strong in the electron temperature (T_e) profile against electron cyclotron heating (ECH). The value of χ_i in the ITB region increased with the electron thermal diffusivity (χ_e), indicating existence of clear relation between ion and electron thermal transport. On the other hand, T_i-ITB unchanged or even grew, when stiffness feature was weak in the T_e profile. Density fluctuation level seemed to be unchanged during ECH, however, correlation length became longer for the T_i-ITB degradation case and shorter for the T_i-ITB unchanging case.

1. Introduction

Advanced tokamak plasmas have been developed with internal transport barriers (ITBs) for establishment of a steady-state operation scenario in fusion reactors such as ITER and DEMO [1]. In order to understand applicability of these plasmas to fusion reactor plasmas, it is important to investigate ITB characteristics under reactor relevant conditions. In JT-60U, weak shear plasmas have been optimized mainly using positive ion based neutral beam injection (P-NBI). The P-NBI provides central fuelling and ion dominant heating, which are different from reactor relevant conditions of edge fuelling and electron dominant heating by α particles. Edge fuelling using shallow pellet injection is considered as a fuelling method in a fusion reactor. In JT-60U, high-field-side (HFS) pellet injection has shown deeper deposition than low-field-side (LFS) injection and compatibility with high confinement, while confinement degrades with gas-puffing [2]. However, large perturbation on fusion output is expected in the case of deep penetration. It is important to investigate whether shallow edge fuelling can lead high confinement at high density with small perturbation or not. Electron heating using electron cyclotron heating (ECH) has induced degradation of the ion temperature (T_i) ITB in JT-60U weak shear plasmas [3]. It is important to investigate mechanisms responsible for the T_i-ITB degradation from a viewpoint of relation to density fluctuations, which dominates anomalous transport.

In this paper, effects of edge fuelling and ECH on ITB were investigated in weak shear

plasmas on JT-60U. In order to investigate impacts of edge fuelling on ITB with various fuelling profiles, Supersonic Molecular Beam Injection (SMBI) [4] has been installed in collaboration with CEA-Cadarache [5]. SMBI has intermediate fuelling profiles between those of pellet injection and gas-puffing. For the investigation of density fluctuations during ECH, reflectometer [6] has been developed with scannable frequency for measurement of correlation length. During the ITB formation phase in the JT-60U reversed shear plasmas, it was found that correlation length becomes shorter and fluctuation level is not largely decreased [7], although large decrease in fluctuation level was observed with an external perturbation induced by pellet injection or ECH [8]. Therefore, measurement of correlation length is important in this study. Fast charge exchange recombination spectroscopy system has also been developed with a time resolution of 2.5 ms [9], which is a powerful tool for the investigation of fast T_i response to edge fuelling and ECH.

2. Impacts of edge fuelling on ITB

2.1. Confinement and pedestal with edge fuelling

In order to investigate fuelling profile on ITB, supersonic molecular beam injection (SMBI) has been installed in collaboration with CEA-Cadarache [5]. Injection frequency is less than 10 Hz and duration is ~2 ms /pulse. Gas flow rate was estimated to be ~1.2 Pam^3/pulse at back ground pressure of P_{BK}=6 bar using measurement of increase in gas pressure after SMBI pulses. This gas flow rate is almost the same as number of particles fuelled by a pellet injection in JT-60U. SMBI speed is expected to be 2.2 km/s at the wall temperature of 150°C and P_{BK}=5 bar. Injector heads were installed at both HFS and LFS (see insets in Fig. 1).

Figure 1 shows dependence of the confinement improvement factor over the ITER89P L-mode scaling (H_{89PL}) on the density normalized to the Greenwald density ($\bar{n}_e/n_{GW}$) [10]. The accessible density range with H_{89PL}~2 was extended to $\bar{n}_e/n_{GW}$~0.7 by maintaining the T_i-ITB using the HFS shallow pellet injections with injection speed of 120 m/s. On the other hand, confinement degraded with gas-puffing (including plus pellet injection case) due to significant degradation of the T_i-ITB. In the case with SMBI at P_{BK}=6 bar, density jump was observed as well as the case with pellet injection, as shown in the insets of Fig. 1. Height of the density jump decreased with P_{BK}. In some discharges, high confinement was sustained with SMBI, although achievable density was lower than that with the HFS pellet injection. High confinement tended to be obtained with relatively smaller perturbation induced

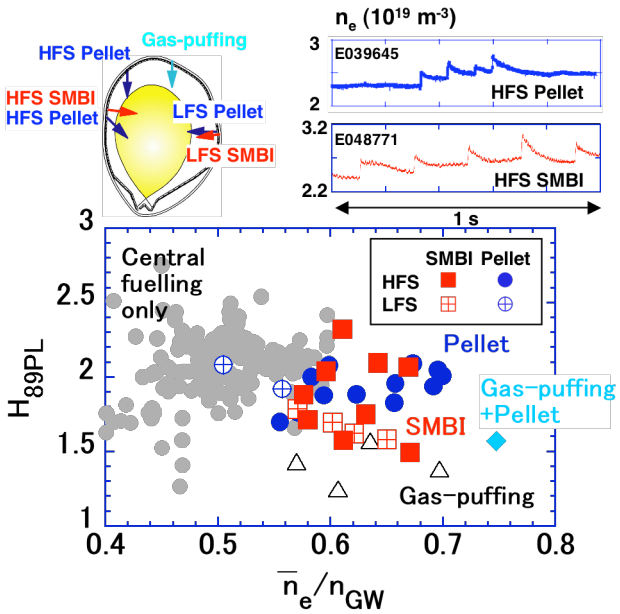

Fig. 1 H_{89PL} as a function of $\bar{n}_e/n_{GW}$. Injection directions and typical time evolutions of the line averaged density for HFS pellet and HFS SMBI (at P_{BK}=6 bar) are shown in the insets.

by SMBI with lower frequency (~5 Hz) and lower P_{BK} (~2-4 bar), although it also depended on target plasma confinement. HFS and LFS SMBI has no clear difference in density dependence of confinement.

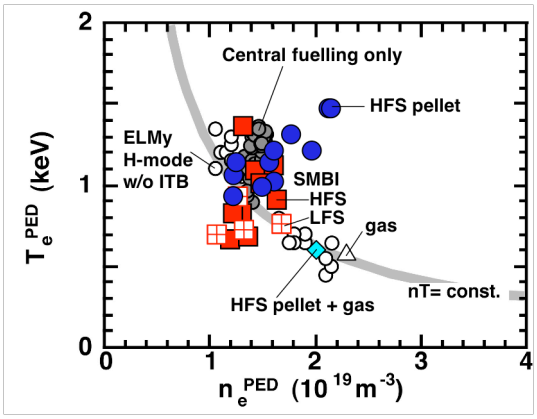

Fig. 2 nT diagram at the pedestal.

The change in confinement is closely related with a strong core-edge linkage [11], that is, improved core confinement (high β_p) enhances the edge pressure and the enhanced edge pressure improves the core confinement. The pedestal pressure was enhanced with the HFS pellet injections, as shown in Fig. 2, with keeping high confinement. However, it decreased with gas-puffing to the same level as that in the standard ELMy H-mode plasmas. In the SMBI case, the pedestal pressure was slightly enhanced in the case with high confinement. However, achieved pedestal pressure with SMBI was smaller than that with HFS pellet injection.

2.2. Fuelling profiles of pellet injection and SMBI

In order to investigate effects of edge fuelling on pedestal pressure and ITB, fuelling profile was estimated for pellet injection and SMBI in this section. The pellet penetration depth was estimated to be λ/a=0.1-0.3 for the HFS pellet injections from the time evolution of electron temperature (T_e), as shown in Fig. 3 (a). Rapid decrease of T_e was observed at r/a=0.84, but not at r/a=0.77. In this case, pellet penetration position was estimated to be r/a=0.77-0.84, which is inside the pedestal top. This penetration depth was deeper than that predicted by the neutral gas shielding (NGS) model [12], as shown in Fig. 3 (b), due to radial movement of ablation material [13, 14]. The deposition profile estimated from the density profile change before and after the HFS pellet injection was consistent with this estimation. On the other hand, the penetration depth for the LFS injection was almost the same as the NGS model calculation. However, fast expel of the pellet ablation material was observed for the LFS injection [2].

Light from the HFS SMBI measured using fast TV with a time resolution of 1/6000 s mainly emitted outside the separatrix even with P_{BK}=6 bar as shown in Fig. 4 (a), indicating that SMBI was almost ionized in the scrape-off layer. However, the edge T_i quickly decreased at r/a~0.8 as shown in Fig. 4 (b) and cold pulse propagated toward the central region.

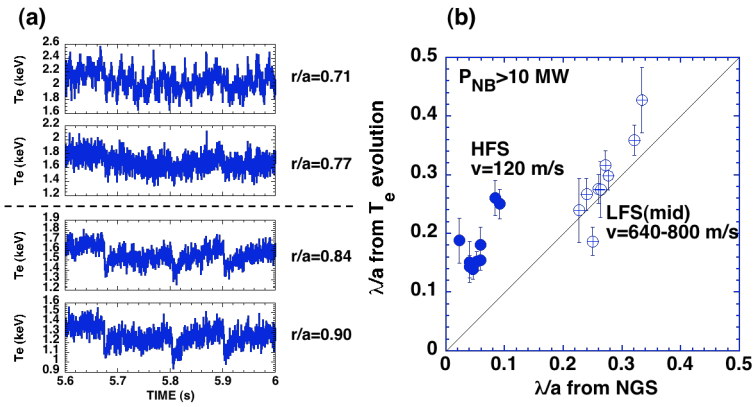

Fig. 3 (a) Time evolution of T_e in the discharge with HFS pellet injection. (b) Comparison of the pellet penetration depth between the measurements and the NGS calculations.

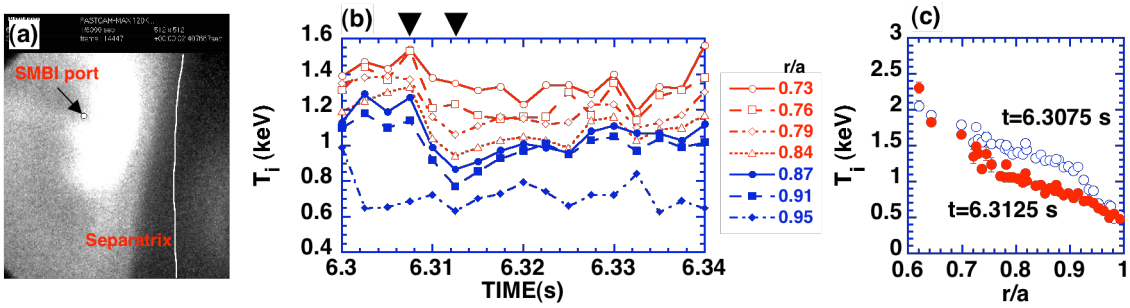

Fig. 4 (a) Fast TV picture for the HFS SMBI at P_{BK}=6 bar. (b) Time evolution of edge T_i. (c) Edge T_i profile before and just after the SMBI (indicated by arrows in (b)).

Therefore, SMBI could directly affect the plasma parameters at r/a~0.8 and also affect through cold pulse propagation inside more. Just after the SMBI, pedestal T_i significantly decreased as shown in Fig. 4 (c). Similar behavior was observed for the LFS SMBI. Therefore, this behavior was not ascribed to the radial movement toward LFS of ablation material observed for the pellet injection. Similar response in T_i was observed at P_{BK}=4 bar, however, response became smaller at P_{BK}= 2 bar. Clear response was not observed in T_e even at P_{BK}= 6 bar. The SMBI speed estimated from the fast TV camera was lower than expected. Ionization front could move slowly towards plasma boundary.

2.3. Time behavior of ion temperature with edge fuelling

Figure 5 shows time evolution of T_i together with plasma store energy and line averaged density for the HFS pellet case, the HFS SMBI with injection frequency of f=10 Hz and P_{BK}=4 bar and the HFS SMBI with f=5 Hz and P_{BK}=4 bar. In the case of pellet injection, although the T_i response to each pellet injection was not measured due to a low time resolution, the T_i decrease was observed in the ITB region. However, it recovered when pellet was not injected in relatively long period (≥300 ms). The plasma stored energy also decreased with pellet injection and recovered after the injection. In the case of SMBI with f=10 Hz, transiently decreased central T_i due to SMBI was not recovered, because next SMBI was injected before recovery. The central T_i and the stored energy largely decreased in this case. In the case of SMBI with f=5 Hz, decreased T_i was not recovered in the early phase. However, it recovered in the latter phase and relatively good ITB was sustained. The decrease in the

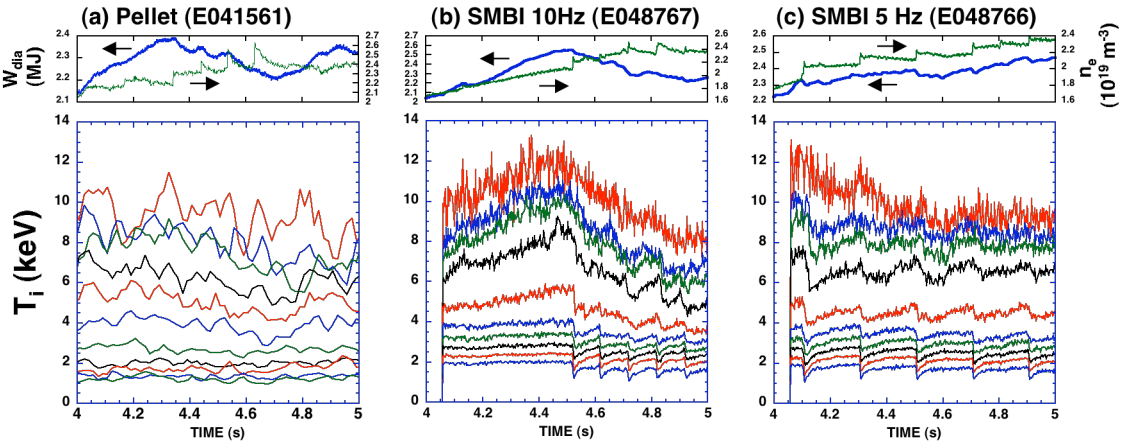

Fig. 5 Time evolution of T_i, plasma store energy and line averaged density for (a) HFS pellet case, (b) HFS SMBI case with f=10 Hz and P_{BK}=4 bar and (c) HFS SMBI case with f=5 Hz and P_{BK}=4 bar.

plasma stored energy was smaller in this case than in other cases. These results indicate that optimization of injection frequency and penetration depth (level of T_i decrease) is important for sustaining high confinement at high density with keeping the good T_i-ITB and enhanced pedestal pressure.

Time behavior of T_i was investigated for understanding mechanisms of the T_i-ITB degradation after SMBI with P_{BK}=6 bar. The value of $\overline{n}_e$, measured with a vertical chord on the magnetic axis, increased by SMBI at t=4.39 s as shown in Fig. 6 (a). Figure 6 (b) shows T_i time evolution after SMBI. Number of injected particles was estimated to be about 5×10^{20} /pulse, which is comparable to pellet injection. The edge T_i quickly decreased as shown in Fig. 6 (b) and cold pulse propagated toward the central region. At t=4.4 s, the T_i decrease has its maximum value at r/a~0.8. The solid lines in Fig. 6 (b) shows the time evolution of T_i calculated using ion thermal diffusivity (χ_i) shown in Fig. 6 (c), which was estimated from the power balance analysis before SMBI. The time evolution was well reproduced using the power balance χ_i. The larger T_i decrease inside the ITB shown in Fig. 6 (c) can be described by the power balance χ_i.

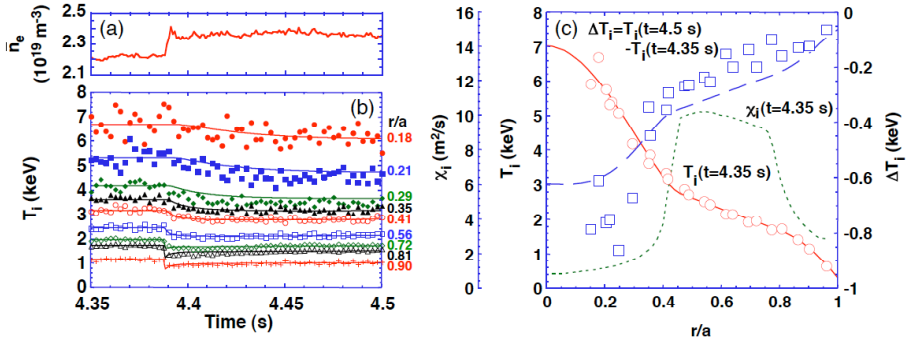

Fig. 6 Time evolution of (a) $\overline{n}_e$ and (b) T_i (symbols) in the discharge with SMBI. Solid lines in (b) show calculated T_i using the power balance χ_i. (c) Profiles of T_i (circles and solid line) and χ_i (dotted line) before SMBI, and difference of T_i (squares: measured and dashed line: simulation) before and after the SMBI.

3. Impacts of ECH on ITB

3.1. Response of T_i-ITB during ECH

The central T_i also decreased during central ECH in the discharges with the plasma current of I_p=0.95-1.0 MA and the toroidal field of B_T=2-3.7 T [3], as shown in Fig. 7. In the discharge shown in Fig. 7, ECH was applied inside of r/a~0.3 with constant NB heating power. The central T_e slightly increased and the central T_i was significantly decreased. The central density also decreased slightly. Although the electron heat flux was increased by a factor of 2.4 with ECH at r/a=0.34, the T_e gradient was almost constant. This stiffness feature was ascribed to the increase in χ_e probably due to enhancement of short-spatial-scale fluctuations such as ETG and high-k TEM. At the same time, ion thermal transport was increased probably due to enhancement of long-spatial-scale fluctuation such as ITG and low-k TEM.

It is important for sustainment of high T_i during electron heating to break this T_e profile stiffness by producing the strong T_e ITB. In fact, increase in central T_e and T_i was observed with strong ITB case as shown in Fig. 8. In this case, central T_e largely increased with ECH

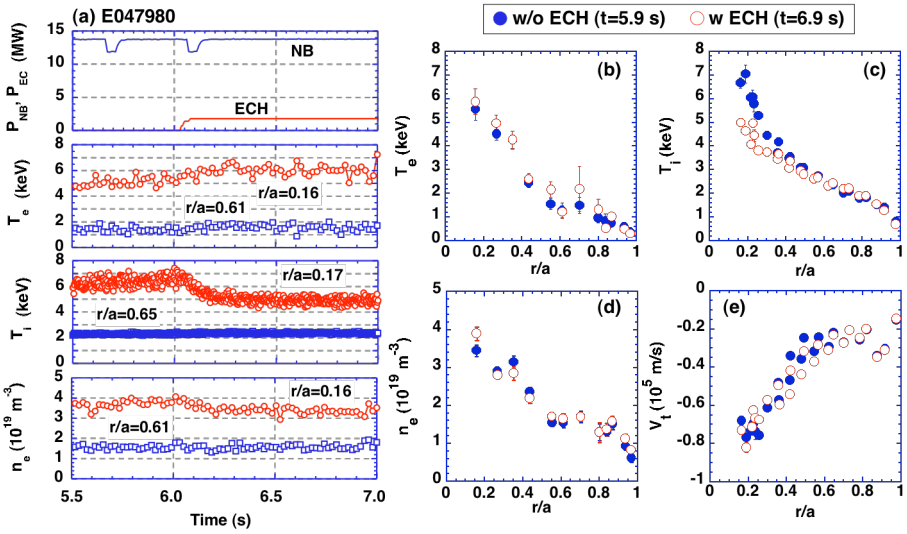

Fig. 7 (a) Waveforms of NB and EC heating power, T_e, T_i and n_e in the T_i-ITB degradation case. Profiles of (b) T_e, (c) T_i, (d) n_e and (e) toroidal rotation without (closed circles) and with (open circles) ECH.

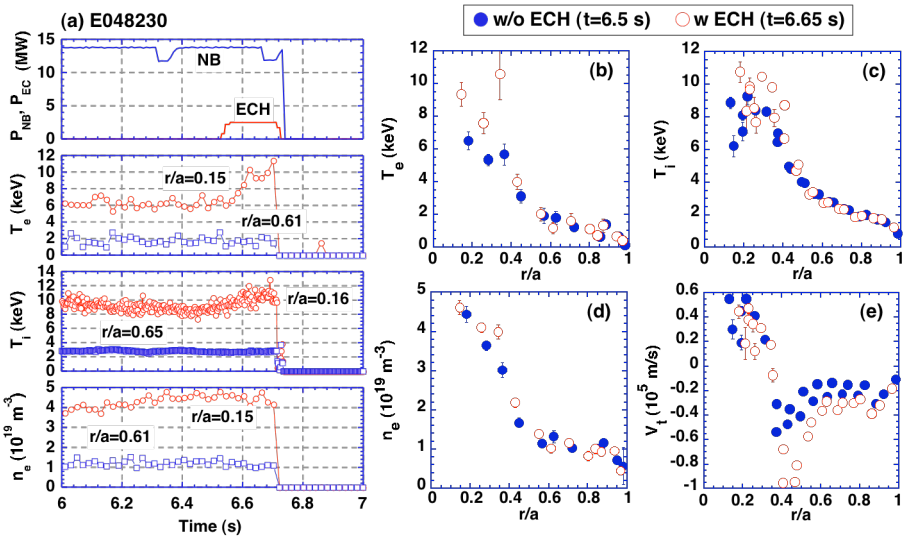

Fig. 8 (a) Waveforms of NB and EC heating power, T_e, T_i and n_e in the T_i-ITB growing case. Profiles of (b) T_e, (c) T_i, (d) n_e and (e) toroidal rotation without (closed circles) and with (open circles) ECH.

and the central T_i also increased with almost constant central density. Finally, plasma disrupted at t=6.72 s due to formation of strong pressure gradient in the ITB region.

3.2. Relation between electron and ion heat transport

Figure 9 shows relation between electron thermal diffusivity (χ_e) and ion thermal diffusivity (χ_i) at r/a=0.34. In the case of T_i-ITB degradation (see Fig. 7) shown by the arrow with solid line, χ_e largely increased with ECH due to the stiffness feature. At the same time, χ_i also increased, indicating existence of clear relation between electron heat transport dominated by short-spatial-scale fluctuations and ion heat transport dominated by long-spatial-scale fluctuations. In the discharges with higher I_p of 1.5 MA, the T_i-ITB degradation was not clear [3]. In these discharges, the stiffness feature was weak compared with that in the lower I_p discharges. Therefore, increase in χ_e, shown by the arrow with dotted line, was smaller and increase in χ_i was also smaller than those in T_i-ITB degradation case with I_p~1.0 MA. However, even with weaker stiffness feature in the discharge with I_p=1.5 MA, χ_i largely

increased in the case shown by the arrow with dashed line, and the T_i-ITB degraded. In this discharge, central T_i was unchanged and the ITB structure was changed from box-type to parabolic-type. Spontaneous structure transition was observed in JT-60U [15]. Mechanism for the degradation of the T_i-ITB might be different from that discussed for lower I_p discharges. In the T_e-ITB growing case, χ_e decreased during ECH as shown by the arrow with dash-dot-dashed line together with χ_i. These results indicate that response to electron heating is different for different confinement regime. It is important to optimize the operation scenario in a fusion reactor considering different response to electron heating.

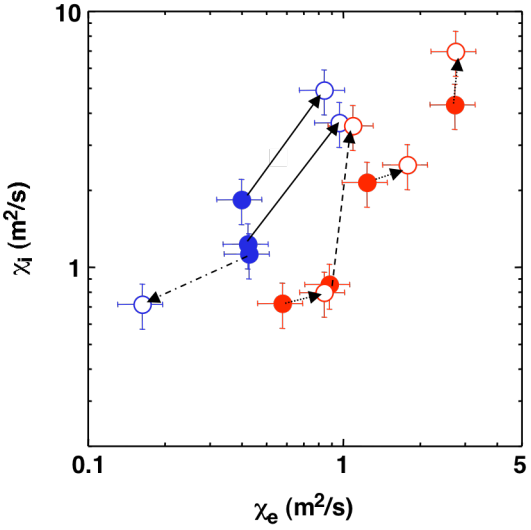

Fig. 9 Relation between χ_e and χ_i (closed circles: without ECH, open circles: with ECH). Blue and red symbols show the data with I_p~1 MA and ~1.5 MA, respectively. Arrows show the time evolution.

3.3. Density fluctuations during ECH

Figure 10 shows spectrograph and correlation of density fluctuation in the frequency range of ITG at r/a~0.3 measured using reflectometer for the T_i-ITB unchanging case and the T_i-ITB degradation case. The spectrum of the scattered wave measured with O-mode reflectomter did not largely changed during ECH in both cases, indicating that the density fluctuation level did not increase with ECH in the T_i-ITB degradation case. Figure 10 also shows comparison of correlation length without and with ECH. The correlation length became shorter for the T_i-ITB unchanging case and longer for the T_i-ITB degradation case. Although dependence of

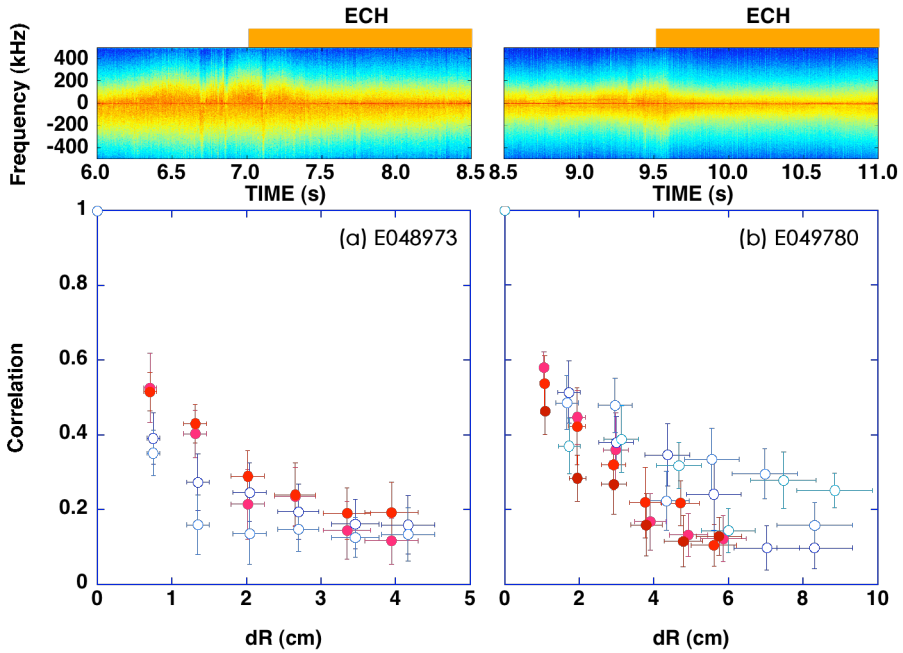

Fig. 10 spectrograph of O-mode reflectometer signal and correlation of density fluctuation at r/a~0.3 for (a) the T_i-ITB unchanging case and (b) the T_i-ITB degradation case. Closed and open symbols show the data without and with ECH, respectively.

χ_i on correlation length might not be simple, these results indicate that ion thermal transport was modified by changing fluctuation property through electron heating using ECH.

Before closing the section, effect of the toroidal rotation (V_t) were briefly discussed, because V_t profile changed with ECH in some cases. The change in χ_e and χ_i was smaller even when the profile of V_t widely changed from co- to ctr-direction using tangential NB without ECH. Therefore, destabilization effect of fluctuations due to reduction of sheared flow induced by the V_t change with ECH played a small role of this ITB degradation.

4. Summary

ITB characteristics have been investigated under reactor relevant condition with edge fuelling and electron heating in JT-60U weak shear plasmas. High confinement was sustained at high density with edge fuelling. Since large perturbation at the edge region leads degradation of ITB and resulting confinement, optimization of the injection frequency and the penetration depth is important. Variety of T_i-ITB response was observed with central ECH depending on the target plasmas. When stiffness feature is strong in T_e profile, T_i-ITB degraded. On the other hand, T_i-ITB unchanged or even grew, when stiffness feature was weak in T_e profile. Density fluctuation level seemed to be unchanged, however, correlation length became longer for the degradation case and shorter for the unchanging case. These results indicate that ion thermal transport was modified by change of fluctuation property through electron heating using ECH. It is important to optimize the operation scenario in a fusion reactor considering ITB responses to edge fuelling and electron heating.

Acknowledgement

The authors would like to acknowledge all people who have contributed to the JT-60 project.

References

[1] Takenaga, H. and the JT-60 Team, Nucl. Fusion **47** (2007) S563.
[2] Takenaga, H. and the JT-60 Team, Phys. Plasmas **8** (2001) 2217.
[3] Ide, S., *et al*., Nucl. Fusion **47** (2007) 1499.
[4] Bucalossi, J., *et al*., Proc. 19th IAEA Fusion Energy Conf. (Lyon, 2002) EX/P4-04.
[5] Takenaga, H., *et al*., Proc. 33rd EPS Conf. Plasma Phys. and Control. Fusion, Vol. **30I** (2006) P-4.112.
[6] Oyama, N. and Shinohara, K., Rev. Sci. Instrum. **73** (2002) 1169.
[7] Nazikian, R., *et al*., Phys. Rev. Lett. **94** (2005) 135002.
[8] Takenaga, H., *et al.*, Plasma Phys. Control. Fusion **48** (2006) A401.
[9] Sakamoto, Y., *et al*., 22nd IAEA Fusion Energy Conf. (Geneva, 2008) EX/1-1.
[10] Takenaga, H. and the JT-60 Team, submitted to J. Nucl. Mater.
[11] Kamada, Y., *et al*., Plasma Phys. Control. Fusion **44** (2002) A279.
[12] Kuteev, B., Nucl. Fusion **35** (1995) 431.
[13] Parks, P. B., *et al*., Phys. Plasmas **7** (2000) 1968.
[14] Strauss, H. R. and Park, W., Phys. of plasmas **5** (1998) 2676.
[15] Ida, K., Proc. 21st IAEA Fusion Energy Conf. (Chengdu, 2006) EX/P4-39.